EurJIC European Journal of Inorganic Chemistry

ChemPubSoc Europe

FULL PAPER

DOI:10.1002/ejic.201300324

Imaging Intracellular Zinc by Using a Glyoxal Bis(4-methyl-4-phenyl-3-thiosemicarbazone) Ligand

Duraippandi Palanimuthu,[a] Sridevi Vijay Shinde,[b] Disha Dayal,[b] Kumaravel Somasundaram,*[b] and Ashoka G. Samuelson*[a]

Keywords: Zinc / Thiosemicarbazones / Imaging agents / Fluorescence / Sensors

The ligand glyoxal bis(4-methyl-4-phenyl-3-thiosemicarbazone) ($GTSCH_2$) is shown to be a selective fluorescence "turn-on" sensor for zinc ions (Zn^{2+}). This sensor is easy to synthesize, exhibits excellent sensitivity and selectivity towards Zn^{2+} over other physiologically relevant cations, and has sub-nanomolar binding affinity. It displays maximum fluorescence response to Zn^{2+} when the metal/ligand ratio is 1:1 and displays stable fluorescence over a broad pH range. The potential of $GTSCH_2$ to image Zn^{2+} inside the cell was demonstrated in MCF-7 cells (human breast cancer cell line) by using flow cytometry and confocal fluorescence microscopy. Cell viability studies reveal that the probe is biocompatible and suitable for cellular applications.

Introduction

Zinc is an essential nutrient for all three domains of life that include archaea, bacteria, and eukaryota.[1] Unlike many other transition-metal ions, redox-inactive Zn^{2+} serves as a cofactor to bring about various catalytic transformations in all six classes of enzymes owing to its excellent Lewis acid properties.[2] It is also the second most abundant transition-metal ion after iron in the human body and plays a pivotal role in the regulation of various metabolic processes, transcription factors, immune functions, ion channels, and neurotransmission.[3] The concentration of zinc in cells is in the millimolar range, but the concentration of the free and loosely bound forms of Zn^{2+} in the cytosol can vary from the picomolar to micromolar range.[4] Whereas the intracellular concentration of Zn^{2+} is tightly controlled by regulating proteins, some cell types, in particular neuronal and pancreatic beta cells, accumulate high concentrations of free Zn^{2+} for a special function such as neurotransmission or insulin secretion.[5] Upsetting Zn^{2+} homeostasis leads to various diseases and disorders such as cancer, diabetes, and many forms of neurodegeneration.[6]

Histochemistry- and radioactivity-based methods have been extensively employed to monitor the concentration of Zn^{2+} in cells, but inherent problems in these methods have motivated chemists and biologists to find alternative tools for better visualization with good optical resolution.[7] Confocal fluorescence microscopy is well suited and has been widely used in recent times for in situ measurements of cellular events such as cellular uptake, localization, trafficking, and efflux processes in real time with spatial and temporal resolution.[8]

To detect Zn^{2+} in a living system, various cell-permeable fluorescent chemosensors having binding affinities for Zn^{2+} in the millimolar to femtomolar range have been developed.[9] Most of them utilize dyes such as cyanine,[10] fluorescein,[11] and rhodamine[12] as fluorophores. Generally, these molecules are functionalized and attached to various groups that would be responsible for binding Zn^{2+} selectively. Whereas most fluorescent sensors have nanomolar to micromolar binding affinities for Zn^{2+},[13] a few of them have sub-nanomolar binding affinity for zinc. These utilize 2-picolylamine-[14] and quinoline-based[15] chelating ligands as receptors because of their high binding affinity for Zn^{2+}. The Zn^{2+} binding group quenches the fluorescence of the dye in its apo form by a through-space photoinduced electron-transfer (PeT) process.[16] However, the fluorescence intensity is enhanced if Zn^{2+} binds to the receptor part, which makes it a turn-on fluorescence sensor.

Though these chemosensors exhibit excellent quantum yields upon complexation with Zn^{2+}, the emission spectra of these complexes overlap with the fluorescence of the free ligand as a result of a small Stokes shift.[17] In addition, these sensors may not be useful for the quantitative determination of Zn^{2+} owing to variations in excitation and emission intensity in local cellular environments, photo-

[a] Department of Inorganic and Physical Chemistry, Indian Institute of Science, Bangalore 560012, India
Fax: +91-80-2360-1552
E-mail: ashoka@ipc.iisc.ernet.in
Homepage: http://ipc.iisc.ernet.in/~ashoka/
[b] Department of Microbiology and Cell Biology, Indian Institute of Science, Bangalore 560012, India
Fax: +91-80-2360-2697
E-mail: skumar@mcbl.iisc.ernet.in
Homepage: http://mcbl.iisc.ernet.in/KumarS/

Supporting information for this article is available on the WWW under http://dx.doi.org/10.1002/ejic.201300324.

bleaching, and uneven dye loading.[18] Some of these difficulties can be overcome by carrying out a ratiometric measurement of the emission intensities of the metal-free ligand and the complexed ligand. Because the ratio between the two emission intensities is not affected by cellular environments, it permits quantitation.[19] The requirement for UV excitation by ratiometric sensors and special instrumentation required to monitor the multiphoton excitation and emission limit their usage in cellular studies.[20]

Thus, developing sensors based on different ligand systems having sub-nanomolar binding affinity for Zn^{2+} and having better selectivity for Zn^{2+} over other physiologically abundant metal ions is of great interest. More importantly, if the fluorescent dye is integrated with the Zn^{2+} receptor and if it has a large Stokes shift upon binding zinc, it would be even better. Such a system was realized by Dilworth et al. who showed the fluorescence of zinc–bis(thiosemicarbazone) complexes and their distribution in various cancer cell lines by using confocal fluorescence microscopy.[21] Recently, Wedd and co-workers reported a water-soluble bis(thiosemicarbazone), which is an absorption-based chemosensor for Zn^{2+} with a high binding affinity of 5.9 nM for zinc.[22] In general, bis(thiosemicarbazones) are easy to synthesize, have good chelating ability with transition-metal ions, and are cell-permeable.[23] We have studied a series of bis(thiosemicarbazone) ligands and their zinc and copper complexes. Among them glyoxal bis(4-methyl-4-phenyl-3-thiosemicarbazone) ($GTSCH_2$) forms a novel trimeric zinc complex $[Zn(GTSC)]_3$ that has been used as a live cell-imaging agent,[24] whereas the corresponding copper complexes have been utilized as anticancer agents.[25]

Here, we show the utility of the $GTSCH_2$ ligand (Figure 1) for imaging intracellular Zn^{2+}. The $GTSCH_2$ probe exhibited excitation and emission in the visible region upon binding Zn^{2+}. It is selective towards Zn^{2+} even in the presence of biologically abundant metal ions and has a binding affinity in the sub-nanomolar range. It is cell-permeable, exerts minimal cytotoxicity, and is capable of imaging intracellular zinc.

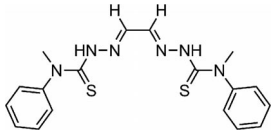

Figure 1. Structure of the glyoxal bis(4-methyl-4-phenyl-3-thiosemicarbazone) ($GTSCH_2$) ligand.

Results and Discussion

The ligand, $GTSCH_2$, was prepared according to a literature procedure, as shown in Scheme S1 (Supporting Information).[24] The Zn^{2+}–$GTSCH_2$ binding behavior was examined by UV/Vis spectroscopy in an aqueous 3-morpholinopropanesulfonic acid (MOPS) buffer (MOPS, 50 mM; NaCl, 100 mM; pH = 7.3) containing 30% DMSO (v/v) at physiological pH. As shown in Figure 2, the UV/Vis spectrum of $GTSCH_2$ exhibits an intense band in the UV region with a maximum at 336 nm ($\varepsilon = 4.0 \times 10^4\ M^{-1}cm^{-1}$). When titrated with increasing concentrations of Zn^{2+} (0–1.4 equiv.), a new band appears in the visible region centered at 458 nm ($\varepsilon = 1.6 \times 10^4\ M^{-1}cm^{-1}$ at 1:1 ratio) with a concomitant decrease in the absorption band at 336 nm ($\varepsilon = 1.0 \times 10^4\ M^{-1}cm^{-1}$ at 1:1 ratio), which is attributed to a ligand-to-metal charge-transfer (LMCT) transition (Figure 2). Appearance of a distinct isosbestic point at 380 nm indicates the formation of single species. Spectral changes indicating the formation of the zinc complex were completed within 5 min. A plot of the absorbance at 458 nm (A_{458}) versus $[Zn^{2+}]/[GTSCH_2]$ resulted in a linear increase in the absorbance until a 1:1 ratio of $GTSCH_2/Zn^{2+}$ was attained, and further incremental additions of Zn^{2+} did not show any enhancement in the absorption (Figure 2). Job's plot analysis further confirmed the 1:1 binding of $GTSCH_2$ and Zn^{2+} in solution (Figure S2, Supporting Information).

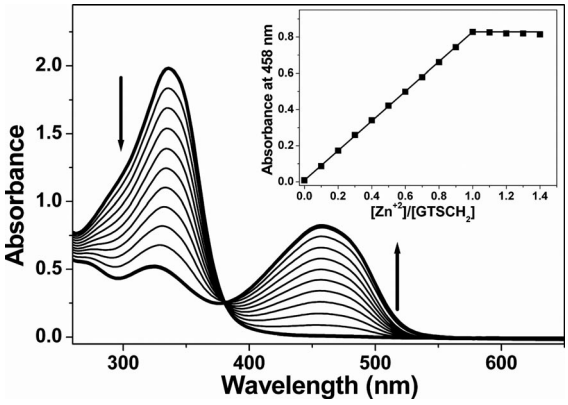

Figure 2. UV/Vis spectra of $GTSCH_2$ (50 μM) in aqueous buffer containing MOPS (MOPS, 50 mM; NaCl, 100 mM; pH = 7.3) and DMSO (30% v/v) in the presence of various concentrations of Zn^{2+} ranging from 0 to 70 μM. Inset plot of A_{458} versus $[Zn^{2+}]/[GTSCH_2]$ shows the 1:1 binding nature.

The fluorescence spectra of $GTSCH_2$ (50 μM) in the absence of and in the presence of Zn^{2+}, are shown in Figure 3 following excitation at 420 nm. Virtually no fluorescence was exhibited by the ligand, but it showed an emission band in the green region of the visible spectrum centered at 560 nm with a large Stokes shift of 102 nm upon complexation with Zn^{2+} (Figure 3). The observed fluorescence intensity increases with increasing concentration of Zn^{2+} until 1 equiv. is reached. Excitation at 380 nm produced a similar emission profile. Thus, fluorescence-based binding analysis is consistent with the UV/Vis absorption experiment. Notably, the addition of an equimolar amount of Zn^{2+} to a solution of $GTSCH_2$ induced a 5.5-fold enhancement in the

fluorescence. The fluorescence quantum yield for the Zn^{2+}–$GTSCH_2$ (1:1) mixture in DMSO was estimated to be 2.0×10^{-3} by using $[Ru(bpy)_3](PF_6)_2$ ($\Phi_f = 42\times10^{-3}$ in water, bpy = 2,2′-bipyridyl) as a standard.[26] However, the fluorescence intensity was quenched by 25% in aqueous phosphate-buffered saline (PBS) solution containing 30% (v/v) of DMSO at pH = 7.3.

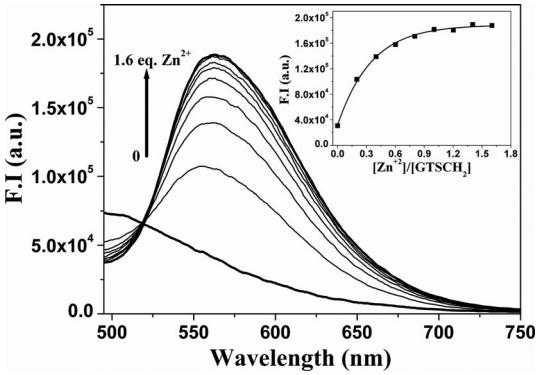

Figure 3. Fluorescence spectra of $GTSCH_2$ (50 μM) in DMSO and changes observed upon addition of a zinc nitrate solution (0–80 μM) in DMSO. Inset plot showing the 1:1 stoichiometric binding nature, as monitored by fluorescence intensity at 560 nm.

The nature of the species present in solution was probed with soft ionization HRMS (ESI–QTOF). The Zn^{2+}–$GTSCH_2$ (1:1 mixture) in DMSO was diluted with methanol for mass spectrometry. Mass spectral analysis in the positive ion mode showed a major peak at *m*/*z* (%) = 447.0395 (100), which was assigned to the Zn(GTSC) monomer (Figure 4). Additionally, the measured isotopic pattern matched the simulated spectrum of the monomer. We observed trace amounts of dimeric (ca. 2%) and trimeric (ca. 0.3%) species in the mass spectrum. This suggested that the ligand forms a 1:1 complex with Zn^{2+} very readily. Signature peaks for $GTSCH_2$ were not observed in the spectrum, which indicates the complete conversion of the ligand into the zinc complex. It also suggests that in solutions of methanol, the major species is the monomer. It is likely that the polar methanol solvent shifts the equilibrium in favor of the monomer.

The binding affinity (K_d) of $GTSCH_2$ for Zn^{2+} was estimated by using competitive binding with ethylene glycol-bis(2-aminoethylether)-*N*,*N*,*N*′,*N*′-tetraacetic acid (EGTA), a suitable competitor having a known dissociation constant of 1 nM to Zn^{2+} at pH = 7.3.[27] The binding event was monitored by UV/Vis spectroscopy (Figure S3, Supporting Information). On the basis of the occupancy of Zn^{2+} in both $GTSCH_2$ and EGTA, the K_d value was estimated to be 0.53 nM in aqueous MOPS (MOPS, 50 mM; NaCl, 100 mM; pH = 7.3) buffer containing 30% (v/v) DMSO (Table S4, Supporting Information). This sub-nanomolar binding affinity makes the probe suitable for cellular applications.

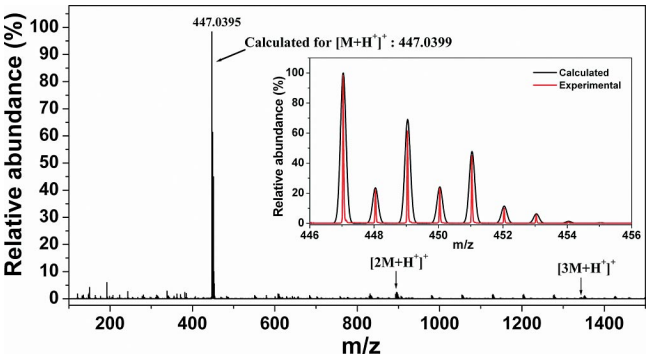

Figure 4. High-resolution mass spectrum of a solution containing $GTSCH_2$ (50 μM) and zinc nitrate (50 μM) in DMSO. The solution was diluted with methanol prior to spectral acquisition. Inset shows the measured spectrum (red line) of the major species and the calculated isotopic distribution profile (black line).

The fluorescence sensitivity of $GTSCH_2$ for Zn^{2+} and other biologically available metal ions was investigated by titration with various metal ions, and the results are shown in Figure 5a and b (blue bar). This fluorescence response study of $GTSCH_2$ (50 μM) with Zn^{2+} (1 equiv.) exhibited "turn-on" fluorescence, whereas other divalent transition-metal ions including Cu^{2+}, Ni^{2+}, Co^{2+}, Fe^{2+}, and Mn^{2+} did not induce fluorescence even at concentrations that were 10-fold higher (0.5 mM). When the experiment was carried out with ubiquitous intracellular metal ions such as K^+, Na^+, Ca^{2+}, and Mg^{2+}, which exist at very high concentrations inside the cell, no significant fluorescence was observed, even at concentrations that were 100-fold higher (5 mM; Figure 5a and b, blue bar).

Metal-ion selectivity was also examined to probe if $GTSCH_2$ could be used as a selective sensor for Zn^{2+} in the presence of other competitive cations found in biological systems. Emission spectra were measured for a 1:1 mixture of $GTSCH_2$ and Zn^{2+} in the presence of other metal ions. The prominent fluorescence enhancement observed upon mixing $GTSCH_2$ and Zn^{2+} remained unchanged, even in the presence of a 100-fold excess of metal ions such as K^+, Na^+, Ca^{2+}, and Mg^{2+} (Figure 5b, red bar). This confirms the excellent selectivity of $GTSCH_2$ for Zn^{2+} over other abundant cations in the cell. Notably, the fluorescence of the zinc complex was completely quenched in the presence of metal ions such as Cu^{2+}, Ni^{2+}, and Co^{2+} when used in 10-fold excess. It is interesting to note that the fluorescence of $GTSCH_2$ in the presence of Zn^{2+} is not quenched by other first-row transition-metal ions such as Mn^{2+} and Fe^{2+} probably as a result of poor binding affinity (Figure 5b, red bar).

To understand the effect of pH on the fluorescence intensity of $GTSCH_2$ in the absence of and in the presence of Zn^{2+} (1 equiv.), the emission spectra were measured as a function of pH (varied from 3 to 11.2) with gradual addition of NaOH. As shown in Figure 6, the ligand itself does not display significant changes in its fluorescence profile in both acidic and basic media. Upon addition of Zn^{2+}

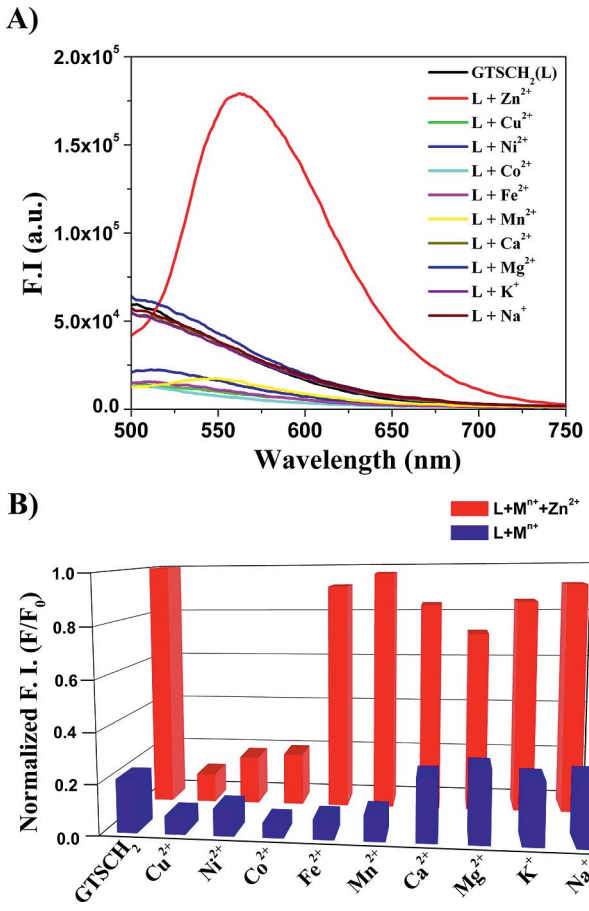

Figure 5. (a) Fluorescence spectra of $GTSCH_2$ (50 μM) in the presence of various metal ions of interest at different concentrations in DMSO following excitation at 420 nm (0.5 mM of Cu^{2+}, Ni^{2+}, Co^{2+}, Fe^{2+}, and Mn^{2+}; 5 mM of Ca^{2+}, Mg^{2+}, K^+, and Na^+). (b) Metal-ion sensitivity and selectivity for $GTSCH_2$. Blue bars represent the fluorescence sensitivity of $GTSCH_2$ (50 μM) to various metal ions (quantified from Figure 5a). Red bars represent the fluorescence response measured after the addition of Zn^{2+} (50 μM) to the indicated metal ion–$GTSCH_2$ (10:1 for transition metal ions and 100:1 for alkali and alkaline earth metal ions) mixture. The response was quantified as F/F_0, for which the integrated emission (500–750 nm) of a 1:1 mixture of Zn^{2+} and $GTSCH_2$ (50 μM) in the absence (F_0) and in the presence of other metal ions (F).

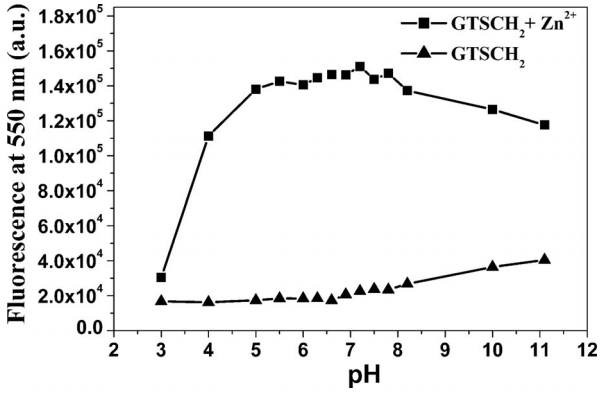

Figure 6. The pH-dependent fluorescence response of $GTSCH_2$ (50 μM) in the absence and in the presence of Zn^{2+} (1 equiv.) in universal pH buffer containing 30% DMSO (v/v). The emission spectra were recorded following excitation at 420 nm, and the fluorescence intensity at 550 nm was plotted against pH increasing from 3.0 to 11.2.

(1 equiv.) to $GTSCH_2$, an approximate sevenfold enhancement in fluorescence was observed at pH = 5.0–7.8. However, the fluorescence intensity decreased dramatically when the pH dropped below 5.0 probably owing to the instability of the complex. The excellent fluorescence response of $GTSCH_2$ with Zn^{2+} in the pH range from 5.0 to 7.8 suggests that the probe may be suitable for imaging zinc in both normal cells and slightly acidic cancer cells.[28]

To test whether $GTSCH_2$ has the ability to form a zinc complex within the cell, MCF-7 (human breast cancer) cells suspended in PBS buffer (pH = 7.4) were incubated either with vehicle [1% DMSO (v/v) in PBS] or with increasing concentrations of $GTSCH_2$ (10–40 μM) at room temperature for 30 min in the presence of or in the absence of added zinc. Cell fluorescence was quantified by using a flow cytometer after excitation at 488 nm. As expected, $GTSCH_2$-treated cells showed no significant increase in fluorescence relative to that shown by vehicle-treated cells at all the concentrations tested (Figure 7a, b). In a separate experiment, the concentration of zinc inside the cell was elevated by supplementing cells with zinc (100 μM) along with pyrithione (20 μM), a zinc-specific ionophore that facilitates the transport of zinc ions across the cell membrane, at room temperature for 30 min. After incubation, the cells were washed thoroughly with fresh PBS buffer to remove extracellular Zn^{2+} and then incubated with $GTSCH_2$ (10–40 μM) for an additional 30 min. The resulting histogram showed a 6.3-fold increase (at 10 μM of $GTSCH_2$) in the cellular fluorescence relative to that shown by cells that were treated with $GTSCH_2$ alone. This is in good agreement with the fluorescence enhancement obtained from zinc titration studies (Figure 3). However, the intensity did not significantly decrease/increase with the addition of increasing amounts of $GTSCH_2$, and this indicates that 10 μM is sufficient to obtain maximal fluorescence. Further incubation of cells with *N*,*N*,*N*′,*N*′-tetrakis(2-pyridylmethyl)ethylenediamine (TPEN, 100 μM), a cell-permeable and high-affinity zinc chelator (K_d = 92 fM), for 10 min resulted in a 3.3-fold quenching (at 10 μM of $GTSCH_2$) of cellular fluorescence, possibly by *trans*-chelation of Zn^{2+} from Zn(GTSC) to TPEN.[29] These results show that $GTSCH_2$ forms a zinc complex by utilizing free zinc in the cells.

The potential of $GTSCH_2$ to enter the cell and image intracellular zinc was examined on MCF-7 cells by using confocal fluorescence microscopy following excitation at 488 nm. The cells were treated with $GTSCH_2$ (10 μM) at 37 °C for 30 min with and without pretreatment with external zinc (100 μM). As shown in Figure 8e–h, treatment of $GTSCH_2$ (10 μM) did not increase the green fluorescence relative to that of vehicle-treated MCF-7 cells (Figure 8a–d). In contrast, the addition of $GTSCH_2$ (10 μM) to cells having transiently increased amounts of Zn^{2+} [pretreated with zinc acetate (100 μM) and pyrithione (20 μM) for

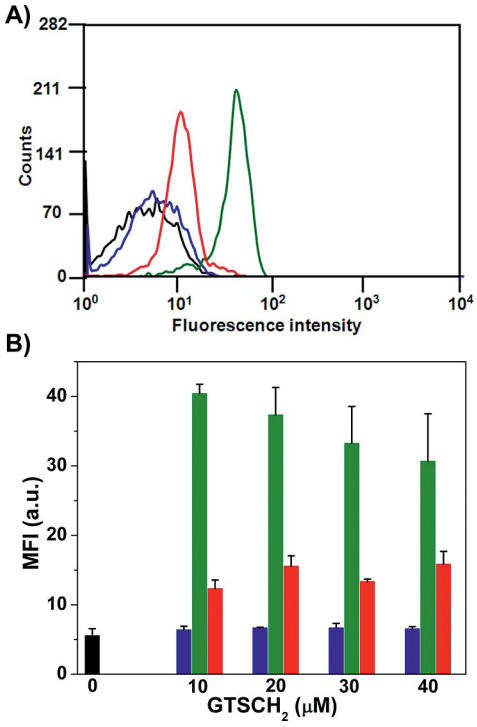

Figure 7. (a) MCF-7 cells treated with 1% DMSO (black line), $GTSCH_2$ (10 μM) before (blue line) and after treatment with zinc acetate (100 μM) along with pyrithione (20 μM) for 30 min (green line). Addition of TPEN (100 μM) to the cells that were preincubated with zinc acetate (100 μM) along with pyrithione (20 μM) for 30 min followed by $GTSCH_2$ (10 μM) for 30 min (red line). The cell fluorescence was measured by using a flow cytometer. (b) Histogram showing mean fluorescence intensity (MFI) from cells that were treated with 1% DMSO (black bar) or different concentrations of $GTSCH_2$ (10, 20, 30, and 40 μM) (blue bar) or zinc acetate (100 μM) along with pyrithione (20 μM) followed by $GTSCH_2$ (10, 20, 30, and 40 μM) (green bar). MFI after addition of TPEN (100 μM) to the cells containing $GTSCH_2$ and Zn^{2+} (red bar).

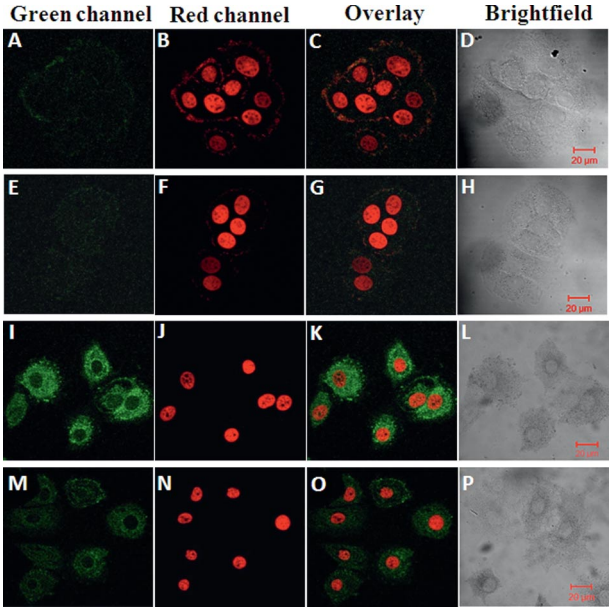

Figure 8. Confocal fluorescence imaging of MCF-7 cells treated with $GTSCH_2$ in the presence of or in the absence of Zn^{2+}. Treatment of MCF-7 cells with 1% DMSO in phenol red-free DMEM media (a–d) or 10 μM $GTSCH_2$ (e–h) at 37 °C for 30 min. Cells supplemented with zinc acetate/pyrithione (5:1) for 30 min and then treated with $GTSCH_2$ (10 μM) at 37 °C for 30 min (i–l). After addition of TPEN (100 μM) to the cells containing $GTSCH_2$ and Zn^{2+} at 37 °C for 30 min (m–p). After all treatments, cells were fixed by using 4% paraformaldehyde, and images were captured immediately in fluorescence and brightfield modes by using a Zeiss confocal fluorescence microscope at 63× magnification. Cells were treated with the nucleus stain propidium iodide (shown in red: b, c, f, g, j, k, n, and o).

30 min] significantly enhanced cellular fluorescence (Figure 8i–l), and the observed fluorescence was quenched by 63% with subsequent addition of TPEN (100 μM; Figure 8m–p). Co-staining of cells with propidium iodide (PI), a nuclear stain, clearly revealed that the probe was localized in the cytoplasm of the cell. All these results confirm that the probe is cell-permeable and that it is capable of monitoring intracellular zinc. Control experiments with the vehicle [1% DMSO (v/v) in phenol-red-free Dulbecco's Modified Eagle's Medium (DMEM)] or zinc acetate along with pyrithione-treated cells in the absence of $GTSCH_2$ did not show any fluorescence, which points to the fact that the observed fluorescence is due to the formation of an intracellular zinc complex with $GTSCH_2$.

Given that imaging probes should be ideally nontoxic, we evaluated the viability of human-derived breast cancer cell line MCF-7, hepatoma cancer cell line HepG2, and immortalized keratinocyte cell line HaCaT by MTT assay after exposure to $GTSCH_2$ for 48 h. The corresponding zinc complex $[Zn(GTSC)]_3$ was included for comparison. Cell viability graphs are shown in Figure 9. The IC_{50} values, corresponding to the cytotoxic activity, obtained from cell viability graphs are shown in Table 1. The IC_{50} values obtained for $GTSCH_2$ are similar to those of its zinc complex in the HaCaT cell line, whereas the IC_{50} values were found to be higher (> 1.6-fold) than those of the zinc complex in the HepG2 and MCF-7 cell lines. Moreover, treatment of cells with 10 μM of $GTSCH_2$, the concentration used for imaging, did not affect the cell viability significantly, as 90–99% of the cells were viable in all the cell lines tested, even after 48 h. Overall, the cell viability studies confirmed that $GTSCH_2$ is biocompatible even for long periods (48 h) and at high concentrations.

Table 1. IC_{50} values[a] as evaluated from an MTT assay in a panel of three cancer cell lines.

Cell line	IC_{50} value [μM]	
	$GTSCH_2$	$[Zn(GTSC)]_3$
MCF-7	>50.0	23.3 ± 6.0
HepG2	53.6 ± 3.5	32.5 ± 1.5
HaCaT	47.5 ± 3.5	47.0 ± 1.4

[a] Data are presented as the mean of three independent experiments.

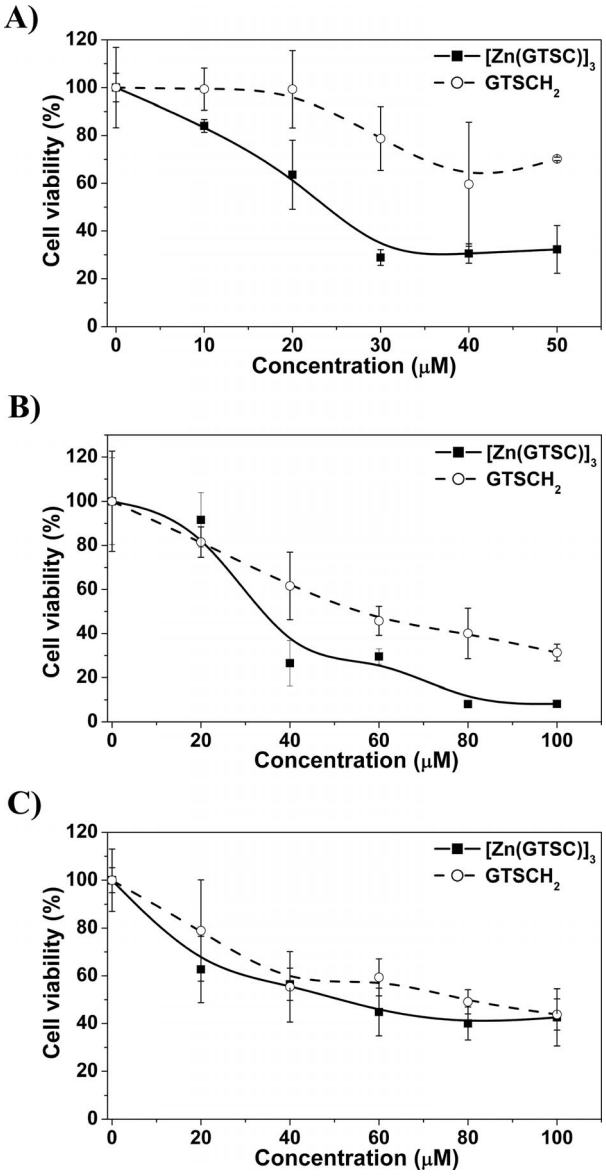

Figure 9. Effect of increasing concentrations of $GTSCH_2$ and $[Zn(GTSC)]_3$ (in zinc) on the cell viability of (a) MCF-7, (b) HepG2, and (c) HaCaT cells after 48 h of treatment. Values are expressed as the mean of triplicates ± the standard deviations of one experiment.

Conclusions

We have shown for the first time that the bis(thiosemicarbazone) ligand $GTSCH_2$ can be used as a zinc-specific sensor. The $GTSCH_2$ probe forms a complex with Zn^{2+} rapidly and selectively. The potential of $GTSCH_2$ in imaging intracellular zinc was demonstrated successfully in the MCF-7 human breast cancer cell line by using flow cytometry and confocal fluorescence microscopy, in which the probe was found to be localized in the cytoplasm. The probe was also found to be noncytotoxic to a range of cell lines. All these properties make $GTSCH_2$ an excellent ligand that is highly suitable for imaging Zn^{2+} in biological systems.

Experimental Section

Materials and Methods: The synthesis and characterization of the $GTSCH_2$ ligand is given in our earlier work.[24] $[Ru(bpy)_3](PF_6)_2$ (bpy = 2,2-bipyridine) and TPEN were synthesized and recrystallized according to literature procedures.[30] MOPS was purchased from SRL, Mumbai, India. EGTA and 2-pyridine *N*-oxide (pyrithione) were procured from Aldrich. Mass spectra were recorded with an Agilent 6538 High accurate-QTOF-LC–MS instrument. All the UV/Vis experiments were carried out with a Perkin–Elmer Lambda 35 instrument. Fluorescence measurements were carried out with a Horiba Jobin Yvon Fluoromax-4 spectrofluorimeter. All solutions and buffers were prepared by using purified water from Milli-Q Biocel made by Millipore. For studying the effect of pH, a stock solution of universal buffer (Britton-Robinson buffer) containing 0.04 M of boric acid, phosphoric acid, and acetic acid was prepared according to a literature procedure.[31] The solution was adjusted to the pH range from 3.0 to 11.2 by adding incremental amounts of NaOH (0.2 M). DMEM media, penicillin, and streptomycin were obtained from Sigma (USA). Sterile 96-well, flat-bottomed tissue-culture plates and other plastic ware were purchased from Tarsons (India). Fetal calf serum (FCS) and 3-(4,5-dimethylthiazol-2-yl)-2,5-diphenyltetrazolium bromide (MTT) used for growth inhibition assays were obtained from Sigma Chemical Co. (India).

Flow Cytometry: MCF-7 cells were cultured in DMEM media, trypsinized, washed with PBS (pH = 7.4), and centrifuged. The resulting pellet was resuspended in PBS buffer (pH = 7.4, 0.5 mL) in a FACS tube. Stock solutions of $GTSCH_2$, zinc acetate, pyrithione, and TPEN were prepared in DMSO (HPLC grade). In the first set of experiments, $GTSCH_2$ (10, 20, 30, and 40 μM) was added to the cells and incubated at room temperature for 30 min. In the second set, cells were pretreated with zinc acetate (100 μM) and pyrithione (20 μM). After 30 min of incubation at room temperature, the cells were pelleted by centrifuge, washed with PBS buffer, and resuspended in fresh PBS buffer (0.5 mL). $GTSCH_2$ (10, 20, 30, and 40 μM) was then added, and the cells were incubated at room temperature for an additional 30 min. In the third set of experiments, the same conditions used for the second set were used. TPEN was then added, and the cells were incubated for another 10 min. In a control experiment, DMSO [1% (v/v) in PBS] was added, and the cells were incubated for 30 min. Finally, the samples were subjected to flow cytometry by using Beckman Coulter CyAn flow cytometer analysis, and the fluorescence was acquired in the FL1 channel for 10000 counts. The forward- and side-scattering parameters were adjusted to keep the background fluorescence to a minimum.

Confocal Fluorescence Imaging: Fluorescence imaging was carried out in MCF-7 cells with and without added Zn^{2+} by using a Zeiss LSM 510 META confocal fluorescence microscope. The cells were grown in DMEM medium in a 6-well dish containing circular cover slips. The next day, the medium was replaced by phenol-red-free DMEM medium (pH = 7.4) containing 10% FCS, penicillin, and streptomycin. The $GTSCH_2$ ligand (10 μM) and DMSO [1% (v/v)] were added to separate wells, and the cells were incubated at 37 °C for 30 min. In a third well, zinc acetate (100 μM) along with pyrithione (20 μM) was added. After incubation at 37 °C for 30 min, the cells were washed with fresh medium and incubated with $GTSCH_2$ (10 μM) at 37 °C for 30 min. The fourth well was given the same treatment as the third but washed with medium, and then TPEN (100 μM) was added, and the cells were incubated at 37 °C for 30 min. After various treatments, the spent medium was removed, and the cells were fixed by using 4% paraformaldehyde. Cells were

then treated with RNAse (200 $\mu g mL^{-1}$ in PBS) for 15 min followed by propidium iodide (1 $\mu g mL^{-1}$ in PBS) for 15 min. Finally, the coverslips were removed and mounted on glass slides, and fluorescence images were captured immediately at an excitation of 488 nm for Zn–$GTSCH_2$ (green) and 543 nm for PI (red). The corresponding brightfield images were also captured.

MTT Assay: MTT assay was carried out for $GTSCH_2$ and its zinc complex on the human breast cancer cell line MCF-7, hepatoma cancer cell line HepG2, and immortalized keratinocyte cell line HaCaT to measure cell viability. An appropriate number of cells was seeded onto a 96-well plate. After 24 h, varying concentrations of either $GTSCH_2$ or $[Zn(GTSC)]_3$ were added, and the cells were incubated in a 37 °C incubator for 48 h. After 45 h of incubation, MTT was added, and the absorbance was read 3 h later on a microplate reader (Molecular devices M5^e) at 550 nm. A graph of concentration versus percentage cell viability gave the IC_{50} value, a concentration at which 50% cell death occurred.

Supporting Information (see footnote on the first page of this article): Synthetic scheme, Job's plot, and binding affinity data.

Acknowledgments

D. P. acknowledges the Council of Scientific and Industrial Research (CSIR), New Delhi, for a senior research fellowship. D. D. thanks the Indian Institute of Science (IISc) for a centenary postdoctoral fellowship. K. S. and A. G. S. thank the Department of Science and Technology (DST), New Delhi, for a research grant. K. S. also thanks the Department of Science and Technology for a J. C. Bose fellowship. We would like to thank the Indian Institute of Science for the imaging facility, the Centre for Imaging Research in Science & Engineering (IRIS), and Ms. Meenakshi for assisting us with the the confocal fluorescence microscopy experiments.

[1] a) S. J. Lippard, J. M. Berg, *Principles of Bioinorganic Chemistry*, University Science Books, Mill Valley, California, USA, **1994**, pp. 139–175; b) C. Andreini, L. Banci, I. Bertini, A. Rosato, *J. Proteome Res.* **2006**, *5*, 3173–3178.
[2] a) J. E. Coleman, *Curr. Opin. Chem. Biol.* **1998**, *2*, 222–234; b) J. M. Berg, Y. Shi, *Science* **1996**, *271*, 1081–1085; c) T. V. O'Halloran, *Science* **1993**, *261*, 715–724.
[3] a) J. E. Coleman, *Annu. Rev. Biochem.* **1992**, *61*, 897–946; b) B. L. Vallee, K. H. Falchuk, *Physiol. Rev.* **1993**, *73*, 79–118; c) T. Fukada, S. Yamasaki, K. Nishida, M. Murakami, T. Hirano, *J. Biol. Inorg. Chem.* **2011**, *16*, 1123–1134.
[4] C. E. Outten, T. V. O'Halloran, *Science* **2001**, *292*, 2488–2492.
[5] a) K. Toth, *Annu. Rev. Nutr.* **2011**, *31*, 139–153; b) N. Wijesekara, F. Chimienti, M. B. Wheeler, *Diabetes Obes. Metab.* **2009**, *11*, 402–414.
[6] a) R. B. Franklin, L. C. Costello, *J. Cell. Biochem.* **2009**, *106*, 750–757; b) A. B. Chausmer, *J. Am. Coll. Nutr.* **1998**, *17*, 109–115; c) C. L. Pao, A. S. Prasad, *Nutr. Res.* **1988**, *8*, 889–897; d) M. P. Cuajungco, G. J. Lees, *Neurobiol. Dis.* **1997**, *4*, 137–169; e) V. Tougu, P. Palumaa, *Coord. Chem. Rev.* **2012**, *256*, 2219–2224.
[7] C. J. Frederickson, G. A. Howell, *The Neurobiology of Zinc*, Alan R. Liss, New York, **1984**.
[8] a) D. W. Domaille, E. L. Que, C. J. Chang, *Nat. Chem. Biol.* **2008**, *4*, 168–175; b) R. McRae, P. Bagchi, S. Sumalekshmy, C. J. Fahrni, *Chem. Rev.* **2009**, *109*, 4780–4827; c) J. W. Lichtman, J. A. Conchello, *Nat. Methods* **2005**, *2*, 910–919.
[9] a) N. C. Lim, H. C. Freake, C. Bruckner, *Chem. Eur. J.* **2005**, *11*, 38–49; b) E. M. Nolan, S. J. Lippard, *Acc. Chem. Res.* **2009**, *42*, 193–203; c) K. Dhara, S. Karan, J. Ratha, P. Roy, G. Chandra, M. Manassero, B. Mallik, P. Banerjee, *Chem. Asian J.* **2007**, *2*, 1091–1100; d) K. Kikuchi, K. Komatsu, T. Nagano, *Curr. Opin. Chem. Biol.* **2004**, *8*, 182–191; e) E. Tomat, S. J. Lippard, *Curr. Opin. Chem. Biol.* **2010**, *14*, 225–230; f) M. D. Pluth, E. Tomat, S. J. Lippard, *Annu. Rev. Biochem.* **2011**, *80*, 333–355; g) K. Komatsu, K. Kikuchi, H. Kojima, Y. Urano, T. Nagano, *J. Am. Chem. Soc.* **2005**, *127*, 10197–10204; h) M. M. Henary, Y. Wu, C. J. Fahrni, *Chem. Eur. J.* **2004**, *10*, 3015–3025; i) R. A. Bozym, R. B. Thompson, A. K. Stoddard, C. A. Fierke, *ACS Chem. Biol.* **2006**, *1*, 103–111; j) Y. Hitomi, C. E. Outten, T. V. O'Halloran, *J. Am. Chem. Soc.* **2001**, *123*, 8614–8615.
[10] a) B. Tang, H. Huang, K. Xu, L. Tong, G. Yang, X. Liu, L. An, *Chem. Commun.* **2006**, 3609–3611; b) K. Kiyose, H. Kojima, Y. Urano, T. Nagano, *J. Am. Chem. Soc.* **2006**, *128*, 6548–6549.
[11] a) G. K. Walkup, S. C. Burdette, S. J. Lippard, R. Y. Tsien, *J. Am. Chem. Soc.* **2000**, *122*, 5644–5645; b) S. C. Burdette, G. K. Walkup, B. Spingler, R. Y. Tsien, S. J. Lippard, *J. Am. Chem. Soc.* **2001**, *123*, 7831–7841; c) C. J. Chang, E. M. Nolan, J. Jaworski, S. C. Burdette, M. Sheng, S. J. Lippard, *Chem. Biol.* **2004**, *11*, 203–210; d) E. M. Nolan, J. W. Ryu, J. Jaworski, R. P. Feazell, M. Sheng, S. J. Lippard, *J. Am. Chem. Soc.* **2006**, *128*, 15517–15528; e) E. M. Nolan, S. J. Lippard, *Inorg. Chem.* **2004**, *43*, 8310–8317.
[12] a) S. L. Sensi, D. Ton-That, J. H. Weiss, A. Rothe, K. R. Gee, *Cell Calcium* **2003**, *34*, 281–284; b) S. L. Sensi, D. Ton-That, P. G. Sullivan, E. A. Jonas, K. R. Gee, L. K. Kaczmarek, J. H. Weiss, *Proc. Natl. Acad. Sci. USA* **2003**, *100*, 6157–6162; c) P. Du, S. J. Lippard, *Inorg. Chem.* **2010**, *49*, 10753–10755.
[13] a) E. L. Que, D. W. Domaille, C. J. Chang, *Chem. Rev.* **2008**, *108*, 1517–1549; b) B. Daniela, J. A. Horowitz, S. J. Lippard, *J. Am. Chem. Soc.* **2011**, *133*, 4101–4114; c) Z. Liu, W. He, Z. Guo, *Chem. Soc. Rev.* **2013**, *42*, 1568–1600.
[14] a) J. E. Kwon, S. Lee, Y. You, K.-H. Baek, K. Ohkubo, J. Cho, S. Fukuzumi, I. Shin, S. Y. Park, W. Nam, *Inorg. Chem.* **2012**, *51*, 8760–8774; b) Z. Xu, J. Yoon, D. R. Spring, *Chem. Soc. Rev.* **2010**, *39*, 1996–2006; c) B. A. Wong, S. Friedle, S. J. Lippard, *Inorg. Chem.* **2009**, *48*, 7009–7011.
[15] a) E. M. Nolan, J. Jaworski, K. I. Okamoto, Y. Hayashi, M. Sheng, S. J. Lippard, *J. Am. Chem. Soc.* **2005**, *127*, 16812–16823; b) Y. Mikata, A. Yamashita, A. Kawamura, H. Konno, Y. Miyamoto, S. Tamotsu, *Dalton Trans.* **2009**, *21*, 3800–3806; c) Y. Zhang, X. Guo, W. Si, L. Jia, X. Qian, *Org. Lett.* **2008**, *10*, 473–476; d) H.-H. Wang, Q. Gan, X.-J. Wang, L. Xue, S.-H. Liu, H. Jiang, *Org. Lett.* **2007**, *9*, 4995–4998.
[16] P. Jiang, Z. Guo, *Coord. Chem. Rev.* **2004**, *248*, 205–229.
[17] a) X. Peng, F. Song, E. Lu, Y. Wang, W. Zhou, J. Fan, Y. Gao, *J. Am. Chem. Soc.* **2005**, *127*, 4170–4171; b) K. Hanaoka, K. Kikuchi, H. Kojima, Y. Urano, T. Nagano, *J. Am. Chem. Soc.* **2004**, *126*, 12470–12476.
[18] a) E. Tomat, S. J. Lippard, *Inorg. Chem.* **2010**, *49*, 9113–9115; b) Z. Wang, M. A. Palacios, G. Zyryanov, P. Anzenbacher, *Chem. Eur. J.* **2008**, *14*, 8540–8546.
[19] a) P. Carol, S. Sreejith, A. Ajayaghosh, *Chem. Asian J.* **2007**, *2*, 338–348; b) K. Komatsu, Y. Urano, H. Kojima, T. Nagano, *J. Am. Chem. Soc.* **2007**, *129*, 13447–13454; c) C. J. Chang, J. Jaworski, E. M. Nolan, M. Sheng, S. J. Lippard, *Proc. Natl. Acad. Sci. USA* **2004**, *101*, 1129–1134.
[20] G. J. Brakenhoff, M. Muller, R. I. Ghauharali, *J. Microsc.* **1996**, *183*, 140–144.
[21] A. R. Cowley, J. Davis, J. R. Dilworth, P. S. Donnelly, R. Dobson, A. Nightingale, J. M. Peach, B. Shore, D. Kerr, L. Seymour, *Chem. Commun.* **2005**, 845–847.
[22] G. Buncic, P. S. Donnelly, B. M. Paterson, J. M. White, M. Zimmermann, Z. Xiao, A. G. Wedd, *Inorg. Chem.* **2010**, *49*, 3071–3073.
[23] a) H. Beraldo, D. Gambino, *Mini-Rev. Med. Chem.* **2004**, *4*, 31–39; b) B. M. Paterson, P. S. Donnelly, *Chem. Soc. Rev.* **2011**, *40*, 3005–3018.
[24] D. Dayal, D. Palanimuthu, S. V. Shinde, K. Somasundaram, A. G. Samuelson, *J. Biol. Inorg. Chem.* **2011**, *16*, 621–632.

[25] D. Palanimuthu, S. V. Shinde, K. Somasundaram, A. G. Samuelson, *J. Med. Chem.* **2013**, *56*, 722–734.
[26] a) J. V. Caspar, T. J. Meyer, *J. Am. Chem. Soc.* **1983**, *105*, 5583–5590; b) S. F. Forgues, D. J. Lavabre, *J. Chem. Educ.* **1999**, *76*, 1260–1264.
[27] A. E. Martell, R. M. Smith (Eds.), *Critical Stability Constants*, vol. 1 (Amino Acids), Plenum Press, New York, **1974**, pp. 469.
[28] J. R. Griffiths, *Br. J. Cancer* **1991**, *64*, 425–427.
[29] a) A. E. Martell, R. M. Smith, *NIST Standard Reference Database 46: NIST Critical Stability Constants of Metal Complexes*, US Department of Commerce, Gaithersburg, **1998**, vol. 5.0; b) A. E. Martell, R. J. Motekaitis, *Determination and Use of Stability Constants*, VCH, Weinheim, **1988**.
[30] a) K. W. Lee, J. D. Slinker, A. A. Gorodetsky, S. Flores-Torres, H. D. Abruna, P. L. Houston, G. G. Malliaras, *Phys. Chem. Chem. Phys.* **2003**, *5*, 2706–2709; b) N. Hirayama, S. Iimuro, K. Kubono, H. Kokusen, T. Honjo, *Talanta* **1996**, *43*, 621–626.
[31] H. T. K. Britton, R. A. Robinson, *J. Chem. Soc.* **1931**, 1456–1462.

Received: March 9, 2013
Published Online: June 4, 2013

